Supplemental Figures

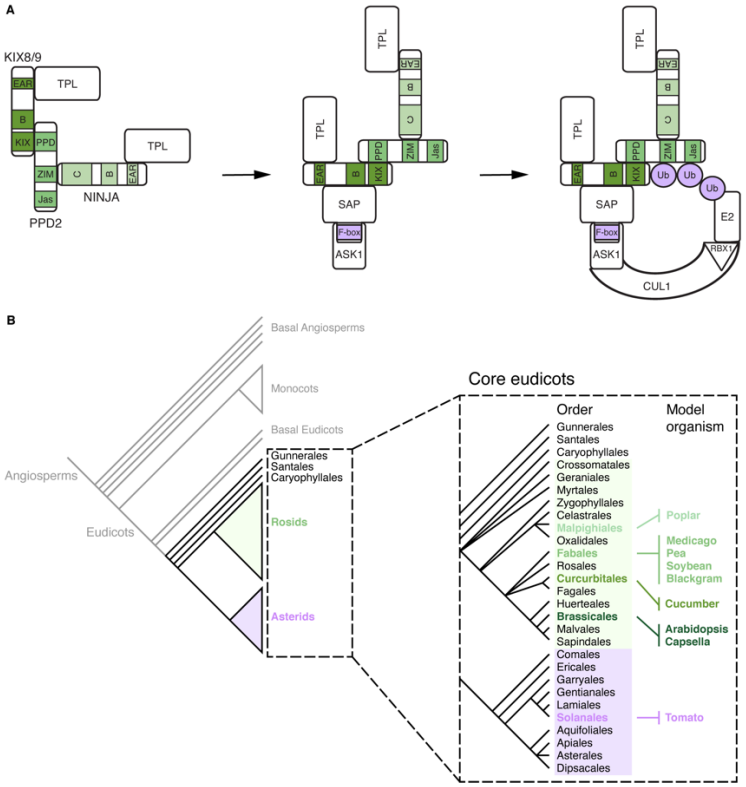

Supplemental Figure S1. A conserved repressor complex regulates leaf growth in distinct eudicot species. (A) The AtPPD2-AtKIX8/AtKIX9 transcriptional repressor complex in *Arabidopsis thaliana*. AtPPD2 interacts with AtKIX8/AtKIX9 and AtNINJA to recruit AtTPL. Interaction of repressor complex members with the E3 ubiquitin ligase $AtSCF^{SAP}$ (comprising the F-box protein AtSAP, AtASK1, AtCUL1, and AtRBX1) leads to the proteasomal degradation of AtKIX8/AtKIX9 and AtPPD2. (B) Model organisms in which KIX, PPD and/or SAP proteins were shown to mediate leaf growth belong to different orders within the rosids, which together with the asterids, make up most of the core eudicot species. Tomato is an asterid model species in which the potential role of these proteins in regulating leaf growth has not been investigated yet. Abbreviations: ASK1, Arabidopsis SKP1; CUL1, CULLIN 1; EAR, ETHYLENE RESPONSE FACTOR (ERF)-ASSOCIATED AMPHIPHILIC REPRESSION; KIX, KINASE-INDUCIBLE DOMAIN

INTERACTING; PPD, PEAPOD; RBX1, RING-BOX 1; SAP, STERILE APETALA; SKP1, S-PHASE KINASE-ASSOCIATED PROTEIN 1; TPL, TOPLESS; Ub, ubiquitin; ZIM, ZINC-FINGER PROTEIN EXPRESSED IN INFLORESCENCE MERISTEM.

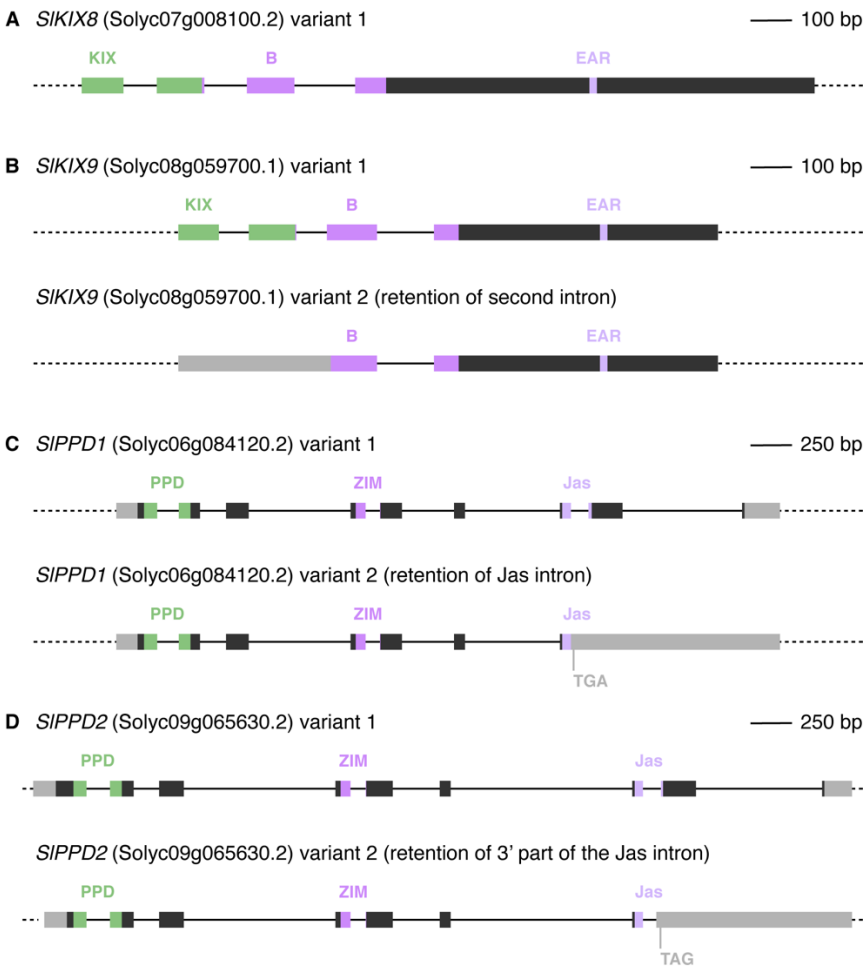

Supplemental Figure S2. Splice variants of *SlKIX8*, *SlKIX9*, *SlPPD1*, and *SlPPD2*. Dark grey boxes represent exons, solid lines represent introns and light grey boxes represent UTRs. Green and purple boxes represent encoded protein domains. No alternative splicing was observed for *SlKIX8* (A). Retention of the second *SlKIX9* intron (B) could lead to the use of a downstream start codon, excluding the sequence that encodes the N-terminal KIX domain. The splice variants of *SlPPD1* (C) and *SlPPD2* (D) display retention of the Jas intron and part of the Jas intron, respectively, which is located between the two exons that encode the Jas domain. These alternative splicing events generate premature stop codons. Abbreviations: UTR, untranslated region.

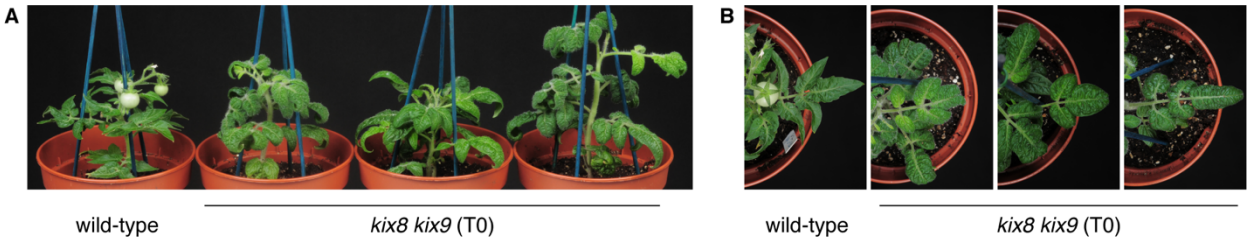

Supplemental Figure S3. Regenerated tomato *kix8 kix9* plants display a rippled, dome-shaped leaf phenotype. (A−B) Wild-type and regenerated *kix8 kix9* plants were photographed from the front (A) and the top (B). Primary transformants transferred from rooting medium were grown in soil for 10 weeks under 16:8 photoperiods with daytime and nighttime temperatures of 26–29°C and 18–20°C, respectively.

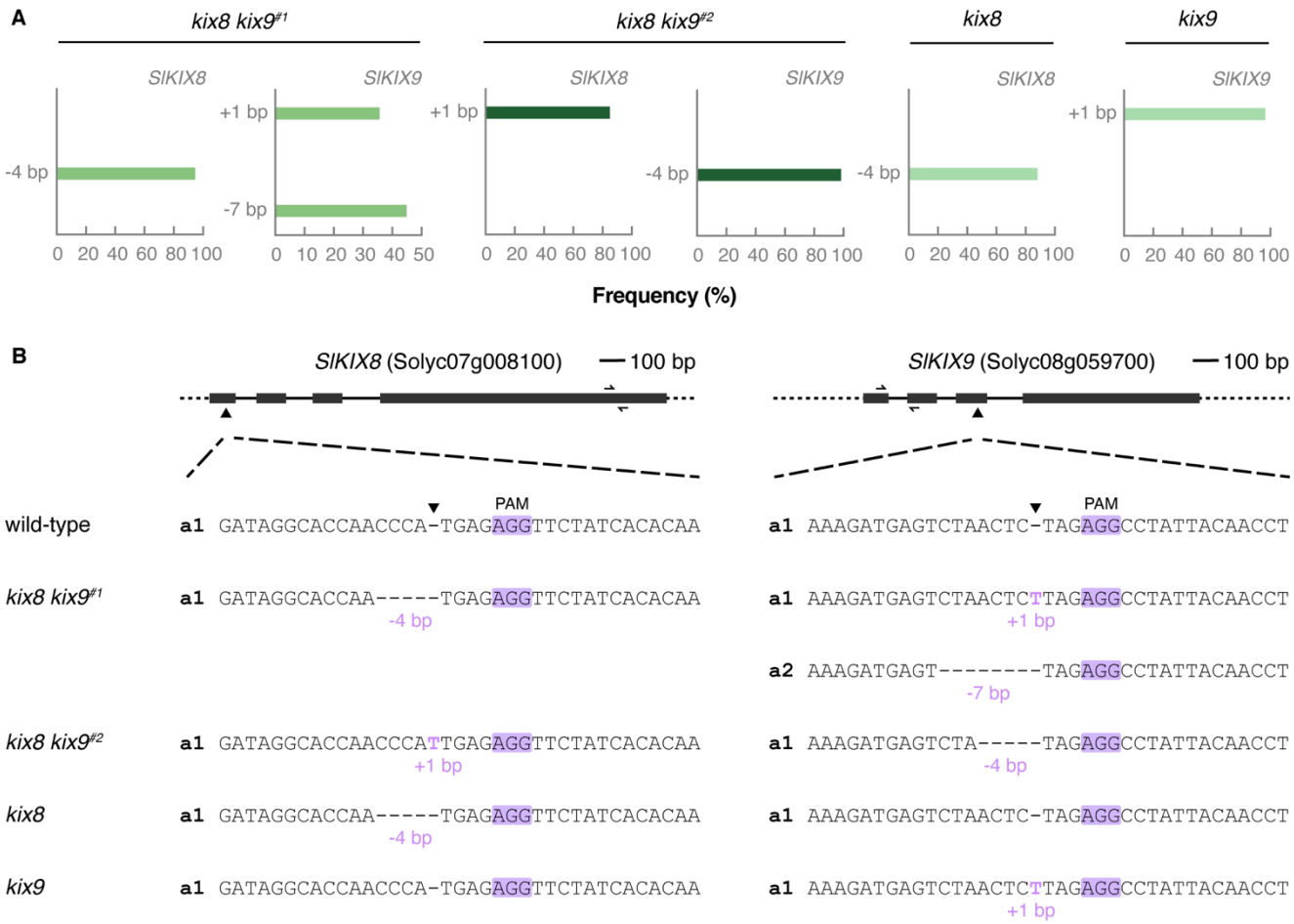

Supplemental Figure S4. CRISPR-Cas9 mutations in double *kix8 kix9* (T1) and single *kix8*, and single *kix9* tomato knockout lines. (A) ICE analysis of genomic sites targeted by the guide RNAs. Targeted genomic regions were PCR amplified and sequenced by Sanger sequencing. Based on the sequence chromatograms, ICE analysis visualized the indel spectrum and calculated the frequency of each indel. (B) Schematic representation of *SlKIX8* and *SlKIX9* with location of the CRISPR-Cas9 cleavage sites. Dark grey boxes represent exons and solid lines represent introns. Cas9 cleavage sites for guide RNAs are indicated with arrowheads. Half arrows indicate the position of primers used for qPCR analysis. Allele sequences are shown for two independent *kix8 kix9* lines, one *kix8* line, and one *kix9* line. Abbreviations: a, allele; PAM, protospacer adjacent motif.

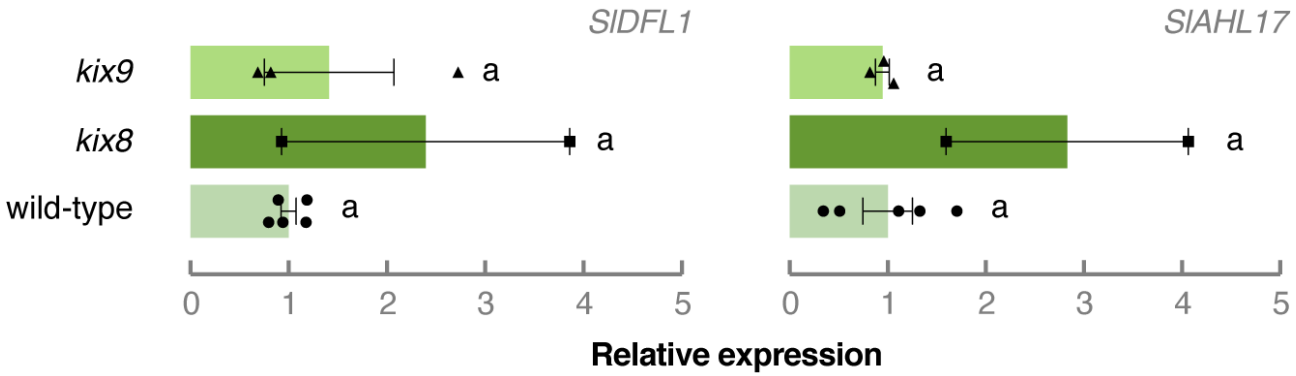

Supplemental Figure S5. Single *kix8* and *kix9* mutants do not display significant upregulation of putative SlPPD target genes. Relative expression of *SlDFL1*, *SlAHL17* in terminal leaflets of not fully developed leaves analyzed by qPCR. The terminal leaflet from the second leaf (from the top) was harvested from plants grown in soil for 3 weeks under 16:8 photoperiods with daytime and nighttime temperatures of 26–29°C and 18–20°C, respectively. Bars represent mean expression relative to the mean of wild-type expression values. Error bars denote standard error (n = 2–5). Individual wild-type (●), *kix8* (■), *kix9* (▲) values are shown. Statistical significance was determined by ANOVA followed by Tukey post-hoc analysis ($P < 0.05$; indicated by different letters).

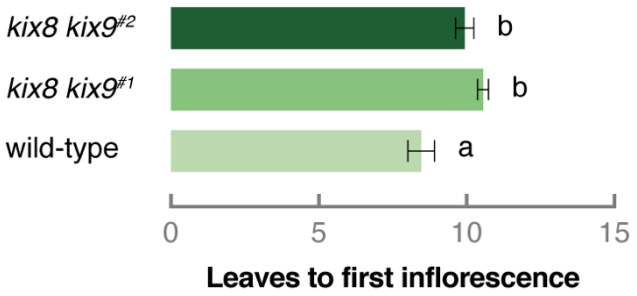

Supplemental Figure S6. Tomato *kix8 kix9* plants display a delay in flowering time. Plants were grown in soil under 16:8 photoperiods with daytime and nighttime temperatures of 26–29°C and 18–20°C, respectively. Bars represent mean number of leaves produced before initiation of the first inflorescence. Error bars denote standard error (n = 15–16). Statistical significance was determined by ANOVA followed by Tukey post-hoc analysis ($P < 0.05$; indicated by different letters).

Supplemental Tables

Supplemental Table S1. Tomato *kix8 kix9* plants display a reduction in plant height.

	wild-type	*kix8 kix9*$^{\#1}$	*kix8 kix9*$^{\#2}$
Height of the primary shoot (cm)	12.33 ± 1.00^{a}	7.83 ± 0.47^{b}	7.83 ± 0.22^{b}
Height of the main shoot (cm)	20.33 ± 1.68^{a}	13.58 ± 0.84^{b}	12.67 ± 0.64^{b}
Internode length (cm)	2.50 ± 0.19^{a}	1.22 ± 0.09^{b}	1.19 ± 0.06^{b}

Plants were grown in soil for 4 months under 16:8 photoperiods with daytime and nighttime temperatures of 26–29°C and 18–20°C, respectively. Data are mean ± standard error (n = 12). Statistical significance was determined by ANOVA followed by Tukey post-hoc analysis ($P < 0.05$; indicated by different letters).

Supplemental Table S2. Normalized expression of *SlKIX8*, *SlKIX9*, *SlPPD1*, *SlPPD2*, *SlDFL1*, *SlAHL17*, and *SlAP2d* in different tomato organs and developmental stages (cultivar Micro-Tom) used to generate heat maps in Figure 4, A and B.

			Flower		Fruit peel					Fruit flesh					Seed				
	Root	Leaf	Bud	Petal	IG	MG	BR	OR	RR	IG	MG	BR	OR	RR	IG	MG	BR	OR	RR
KIX8	0.040	0.022	0.061	0.079	0.026	0.011	0.013	0.006	0.0134	0.044	0.018	0.022	0.008	0.009	0.120	0.078	0.103	0.179	0.158
KIX9	0.053	0.008	0.021	0	0	0	0	0	0	0	0.001	0	0	0	0.001	0.001	0	0	0
PPD1	0.006	0.017	0.041	0.010	0.010	0.006	0.010	0	0	0.020	0.003	0.005	0	0.002	0.035	0.015	0.011	0.006	0.012
PPD2	0.098	0.035	0.090	0.039	0.020	0.034	0.060	0.050	0.080	0.040	0.020	0.037	0.029	0.061	0.066	0.069	0.074	0.053	0.082
DFL1	0.031	0.067	0.190	0.033	0.007	0.011	0	0	0	0.010	0.007	0.007	0.019	0.004	0.049	0.165	0.633	0.980	0.450
AHL17	0.123	0	0.098	0.043	0.010	0.065	0.040	0.110	0.310	0.010	0.017	0.015	0.041	0.253	0.071	0.158	0.533	0.925	0.405
AP2d	0.164	0.046	0.092	0.024	0.542	1.108	0.520	0	0	0.120	0.223	0.323	0.036	0.003	0.032	0.038	0.019	0.023	0.025

Expression data was obtained from TomExpress (Zouine *et al.*, 2017). Abbreviations: IG, immature green; MG, mature green; BR, breaker; OR, orange; RR, red ripe.

Supplemental Table S3. Tomato *kix8 kix9* plants display a reduction in axillary shoot formation

	wild-type	*kix8 kix9*$^{\#1}$	*kix8 kix9*$^{\#2}$
Inflorescence parameters:			
Main shoot			
Number of inflorescences	2.75 ± 0.18^{a}	2.75 ± 0.18^{a}	2.83 ± 0.24^{a}
Number of flowers per inflorescence	14.24 ± 1.09^{a}	10.26 ± 0.93^{b}	7.36 ± 0.84^{c}
Number of pollinated flowers per inflorescence	8.16 ± 1.05^{a}	4.72 ± 0.88^{b}	3.14 ± 0.62^{b}
Pollinated/total number of flowers per inflorescence (%)	57.01 ± 7.04^{a}	42.25 ± 7.54^{a}	45.53 ± 6.32^{a}
Axillary shoots			
Number of inflorescences	5.17 ± 0.49^{a}	2.25 ± 0.37^{b}	2.75 ± 0.13^{b}
Fruit parameters:			
Main shoot and axillary shoots			
Green fruit biomass (g)	0.93 ± 0.60^{a}	1.38 ± 1.11^{a}	1.59 ± 0.99^{a}
Breaker–orange fruit biomass (g)	1.50 ± 0.77^{a}	2.11 ± 0.89^{a}	3.90 ± 1.21^{b}
Red fruit biomass (g)	2.01 ± 0.96^{a}	3.68 ± 1.16^{b}	4.65 ± 1.27^{c}
Main shoot			
Breaker–red fruit pericarp thickness (mm)	1.55 ± 0.09^{a}	2.86 ± 0.12^{b}	3.23 ± 0.09^{c}
Breaker–red fruit pericarp thickness/radius (%)	19.46 ± 0.42^{a}	29.18 ± 0.78^{b}	29.30 ± 0.37^{b}
Fruit yield parameters:			
Main shoot			
Number of green fruits	1.58 ± 0.63^{a}	4.58 ± 0.74^{b}	1.50 ± 0.38^{a}
Number of breaker–orange fruits	1.75 ± 0.80^{a}	1.58 ± 0.45^{a}	0.75 ± 0.30^{a}
Number of red fruits	18.92 ± 1.96^{a}	8.92 ± 0.53^{b}	8.00 ± 0.72^{b}
Total fruit number	22.25 ± 2.06^{a}	15.08 ± 1.23^{b}	10.25 ± 0.76^{b}
Green fruit yield (g)	2.09 ± 1.06^{a}	6.81 ± 1.70^{b}	2.50 ± 0.79^{ab}
Breaker–orange fruit yield (g)	1.42 ± 0.63^{a}	3.51 ± 1.02^{a}	2.76 ± 1.11^{a}
Red fruit yield (g)	39.25 ± 4.71^{a}	31.75 ± 2.27^{a}	35.50 ± 1.91^{a}
Total fruit yield (g)	42.77 ± 4.99^{a}	42.07 ± 3.06^{a}	40.76 ± 2.05^{a}
Axillary shoots			
Number of green fruits	16.00 ± 3.57^{a}	0.42 ± 0.19^{b}	0.25 ± 0.13^{b}
Number of breaker–orange fruits	5.42 ± 1.37^{a}	0.50 ± 0.50^{b}	0.00 ± 0.00^{b}
Number of red fruits	1.67 ± 0.57^{a}	0.42 ± 0.34^{a}	0.92 ± 0.26^{a}
Total fruit number	23.08 ± 4.56^{a}	1.33 ± 0.91^{b}	1.17 ± 0.27^{b}
Green fruit yield (g)	12.25 ± 1.33^{a}	0.51 ± 0.27^{b}	0.28 ± 0.19^{b}
Breaker–orange fruit yield (g)	8.00 ± 2.00^{a}	1.25 ± 1.25^{b}	0.00 ± 0.00^{b}
Red fruit yield (g)	3.58 ± 1.36^{a}	0.92 ± 0.75^{a}	4.00 ± 1.27^{a}
Total fruit yield (g)	23.83 ± 2.78^{a}	2.68 ± 2.17^{b}	4.28 ± 1.29^{b}
Main shoot and axillary shoots			
Number of green fruits	17.58 ± 3.54^{a}	5.00 ± 0.72^{b}	1.75 ± 0.39^{b}
Number of breaker–orange fruits	7.17 ± 1.78^{a}	2.08 ± 0.56^{b}	0.75 ± 0.30^{b}
Number of red fruits	20.58 ± 1.61^{a}	9.33 ± 0.43^{b}	8.92 ± 0.69^{b}
Total fruit number	45.33 ± 3.75^{a}	16.42 ± 0.96^{b}	11.42 ± 0.71^{b}
Green fruit yield (g)	14.34 ± 1.52^{a}	7.32 ± 1.75^{b}	2.78 ± 0.93^{b}
Breaker–orange fruit yield (g)	9.42 ± 2.21^{a}	4.76 ± 1.34^{ab}	2.76 ± 1.11^{b}
Red fruit yield (g)	42.83 ± 3.72^{a}	32.67 ± 1.87^{b}	39.50 ± 2.10^{ab}
Total fruit yield (g)	66.60 ± 3.18^{a}	44.75 ± 2.37^{b}	45.04 ± 2.24^{b}
Seed yield parameters:			
Main shoot			
Number of seeds in red fruit	11.42 ± 8.54^{a}	6.92 ± 5.30^{b}	5.95 ± 4.73^{b}
Seed area in red fruit (mm^2)	5.98 ± 0.84^{ab}	6.11 ± 1.45^{a}	5.50 ± 1.35^{b}

Plants were grown in soil for 3.5–4.5 months under 16:8 photoperiods with daytime and nighttime temperatures of 26–29°C and 18–20°C, respectively. Inflorescence parameters were measured and fruits were harvested from each genotype when the ratio of ripe to unripe fruits on the main shoot was 60–85%. Data are mean ± standard error (n = 12). Statistical significance was determined by ANOVA followed by Tukey post-hoc analysis ($P < 0.05$; indicated by different letters).

Supplemental Table S4. Oligonucleotides used in this study.

Oligonucleotide	Sequence (5'–3')	Orientation	Description	SolycID
Oligonucleotides for Y2H/Y3H constructs:				
LAPAU2860	GGGGACAAGTTTGTACAAAAAAGCAGGCTCCATGCCTAGACCAGGACCCAG	Forward	amplification of *KIX8*	Solyc07g008100.2
LAPAU2994	GGGGACCACTTTGTACAAGAAAGCTGGGTCTCMCAAACCTGGCCTTTTCATTTG	Reverse		
LAPAU2862	GGGGACAAGTTTGTACAAAAAAGCAGGCTCCATGCCTAAATCTACAAGAGC	Forward	amplification of *KIX9*	Solyc08g059700.1
LAPAU2863	GGGGACCACTTTGTACAAGAAAGCTGGGTCTCMGGACTTGAATTTGTTAAAATG	Reverse		
LAPAU2856	GGGGACAAGTTTGTACAAAAAAGCAGGCTCCATGCCGCCGGAAGAAACAG	Forward	amplification of *PPD1*	Solyc06g084120.2
LAPAU2857	GGGGACCACTTTGTACAAGAAAGCTGGGTCTCMCTTTCTAACATCTCTGTC	Reverse		
LAPAU2858	GGGGACAAGTTTGTACAAAAAAGCAGGCTCCATGTCGCTGGAACAAACTG	Forward	amplification of *PPD2*	Solyc09g065630.2
LAPAU2859	GGGGACCACTTTGTACAAGAAAGCTGGGTCTCMCTCTTTACCATCTTTG	Reverse		
COMBI6198	GGGGACAAGTTTGTACAAAAAAGCAGGCTCCATGTCGTCTTCACAATCACCACCATC	Forward	amplification of *SAP*	Solyc05g041220.2
COMBI6199	GGGGACCACTTTGTACAAGAAAGCTGGGTTCACTATTGTGCACCAAAGTCCCACAAATG	Reverse		
Oligonucleotides for CRISPR-Cas9 constructs:				
LAPAU2582	ATTGATAGGCACCAACCCATGAG	Forward	*KIX8* gRNA target site	Solyc07g008100.2
LAPAU2583	AAACCTCATGGGTTGGTGCCTAT	Reverse		
LAPAU2580	ATTGAAAGATGAGTCTAACTCTAG	Forward	*KIX9* gRNA target site	Solyc08g059700.1
LAPAU2581	AAACCTAGAGTTAGACTCATCTTT	Reverse		
Oligonucleotides for the identification of CRISPR-Cas9 mutants:				
LAPAU3075	TCCCTCATCAGATCCACCTC	Forward	amplification of *Cas9*	–
LAPAU3076	CTGAAACCTGAGCCTTCTGG	Reverse		
LAPAU2783	CCCCTCCAAAACACTCATGT	Forward	amplification of *KIX8* gRNA target region	Solyc07g008100.2
LAPAU2784	GAGCAGTACAAATGAGCAGCA	Reverse		
LAPAU2785	GCTGAAGAAATTATGTATTCCAAAGC	Forward	amplification of *KIX9* gRNA target region	Solyc08g059700.1
LAPAU2786	CCCGAGAAGTTTCACTCGAA	Reverse		
Oligonucleotides for gene expression analysis by qPCR:				
COMBI5428	CCTCCGTTGTGATGTAACTGG	Forward	amplification of *CAC*	Solyc08g006960.2
COMBI5429	ATTGGTGGAAAGTAACATCATCG	Reverse		
COMBI5416	ATGGAGTTTTTGAGTCTTCTGC	Forward	amplification of *TIP41*	Solyc10g049850.1
COMBI5417	GCTGCGTTTCTGGCTTAGG	Reverse		
COMBI7162	ACCATCGAAGAGTCTCTCAACAGC	Forward	amplification of *DFL1*	Solyc07g063850.2
COMBI7163	CAATGGATTTGTCTGAGGCACGAC	Reverse		
COMBI7168	CTGTCATTTGCCGTCGGATGTG	Forward	amplification of *AHL17*	Solyc04g076220.2
COMBI7169	AGTAAGGCGGTGGTTGTGGTTG	Reverse		
COMBI7158	TGCATAGTCAGGTCGGAACAACG	Forward	amplification of *AP2d*	Solyc11g072600.1
COMBI7159	TGGTAGCCGGAGTTGAGAATCC	Reverse		
COMBI7188	AGGCTGTGTCTACCAGCAAAGAC	Forward	amplification of *KIX8*	Solyc07g008100.2
COMBI7189	TTGCAACCCGGAGTGACTGTTG	Reverse		
COMBI7190	AGACACCAACCAATCAGAGGTTCC	Forward	amplification of *KIX9*	Solyc08g059700.1
COMBI7191	TGCTGAGCCATGAACCTCATTCAC	Reverse		